

This information is current as of February 26, 2022.

Decreased T Follicular Regulatory Cell/T Follicular Helper Cell (T_{FH}) in Simian Immunodeficiency Virus–Infected Rhesus Macaques May Contribute to Accumulation of T_{FH} in Chronic Infection

Ankita Chowdhury, Perla Maria Estrada Del Rio, Greg K. Tharp, Ronald P. Tribble, Rama R. Amara, Ann Chahroudi, Gustavo Reyes-Teran, Steven E. Bosinger and Guido Silvestri

J Immunol 2015; 195:3237–3247; Prepublished online 21 August 2015;

doi: 10.4049/jimmunol.1402701

<http://www.jimmunol.org/content/195/7/3237>

Supplementary Material <http://www.jimmunol.org/content/suppl/2015/08/20/jimmunol.1402701.DCSupplemental>

References This article **cites 36 articles**, 11 of which you can access for free at: <http://www.jimmunol.org/content/195/7/3237.full#ref-list-1>

Why *The JI*? [Submit online.](#)

- **Rapid Reviews! 30 days*** from submission to initial decision
- **No Triage!** Every submission reviewed by practicing scientists
- **Fast Publication!** 4 weeks from acceptance to publication

**average*

Subscription Information about subscribing to *The Journal of Immunology* is online at: <http://jimmunol.org/subscription>

Permissions Submit copyright permission requests at: <http://www.aai.org/About/Publications/JI/copyright.html>

Email Alerts Receive free email-alerts when new articles cite this article. Sign up at: <http://jimmunol.org/alerts>



Errata An erratum has been published regarding this article. Please see [next page](#)
or:
[/content/195/12/5843.full.pdf](#)



Decreased T Follicular Regulatory Cell/T Follicular Helper Cell (T_{FH}) in Simian Immunodeficiency Virus–Infected Rhesus Macaques May Contribute to Accumulation of T_{FH} in Chronic Infection

Ankita Chowdhury,* Perla Maria Estrada Del Rio,*[†] Greg K. Tharp,* Ronald P. Tribble,* Rama R. Amara,* Ann Chahroudi,*[‡] Gustavo Reyes-Teran,[†] Steven E. Bosinger,* and Guido Silvestri*

T follicular helper cells (T_{FH}) are critical for the development and maintenance of germinal center (GC) and humoral immune responses. During chronic HIV/SIV infection, T_{FH} accumulate, possibly as a result of Ag persistence. The HIV/SIV-associated T_{FH} expansion may also reflect lack of regulation by suppressive follicular regulatory $CD4^+$ T cells (T_{FR}). T_{FR} are natural regulatory T cells (T_{REG}) that migrate into the follicle and, similar to T_{FH} , upregulate CXCR5, Bcl-6, and PD1. In this study, we identified T_{FR} as $CD4^+CD25^+FOXP3^+CXCR5^+PD1^{hi}Bcl-6^+$ within lymph nodes of rhesus macaques (RM) and confirmed their localization within the GC by immunohistochemistry. RNA sequencing showed that T_{FR} exhibit a distinct transcriptional profile with shared features of both T_{FH} and T_{REG} , including intermediate expression of FOXP3, Bcl-6, PRDM1, IL-10, and IL-21. In healthy, SIV-uninfected RM, we observed a negative correlation between frequencies of T_{FR} and both T_{FH} and GC B cells, as well as levels of $CD4^+$ T cell proliferation. Post SIV infection, the T_{FR}/T_{FH} ratio was reduced with no change in the frequency of T_{REG} or T_{FR} within the total $CD4^+$ T cell pool. Finally, we examined whether higher levels of direct virus infection of T_{FR} were responsible for their relative depletion post SIV infection. We found that T_{FH} , T_{FR} , and T_{REG} sorted from SIV-infected RM harbor comparable levels of cell-associated viral DNA. Our data suggest that T_{FR} may contribute to the regulation and proliferation of T_{FH} and GC B cells in vivo and that a decreased T_{FR}/T_{FH} ratio in chronic SIV infection may lead to unchecked expansion of both T_{FH} and GC B cells. *The Journal of Immunology*, 2015, 195: 3237–3247.

Several key findings over the past few years have energized efforts toward the development of an effective HIV vaccine, including the discovery and characterization of a number of broadly neutralizing Abs (bnAbs) that develop in a subset of HIV-infected individuals. However, the mechanisms involved in shaping Ab responses to immunization with HIV Ags or natural HIV infection remain incompletely understood (1). Importantly, HIV-Env-specific bnAbs develop at relatively late stages of HIV infection and show

peculiar genetic and molecular features, including a high level of divergence from germline predecessors, which indicates that they are the products of extensive somatic hypermutation within germinal centers (GCs), as well as the presence of unusually long CDR3 regions (2). Perplexingly, there appear to be no direct or predictable routes to the development of these bnAbs from the germline predecessors, and it remains unclear whether this process is driven by antigenic mutations and/or escape as opposed to specific intrinsic aspects of the B cell or Th cell response (3). A better understanding of the mechanisms responsible for the development of bnAbs is crucial to harness this type of immunity for HIV prevention and therapy in humans.

T follicular helper cells (T_{FH}) are critical for the development and maintenance of GCs, and competition for survival signals from T_{FH} via molecules such as CD40L and IL-21 is thought to be a key mechanism of selection of high-affinity B cells (4). The regulation of T_{FH} frequency, and by extension the regulation of their impact on GC B cell development and function, is vital to the quality of the humoral immune response (5). Although the presence of too few T_{FH} may lead to abortive GC formation and defective B cell responses, an overexpansion is associated with the prevalence of autoantibodies (6, 7). It is possible that an expansion of T_{FH} also lowers the selection pressure on GC B cells and leads to the emergence of low-affinity B cells (8).

Several studies have shown that T_{FH} accumulate during the chronic stages of HIV/SIV infection. This accumulation occurs even though these cells support high levels of viral replication and represent an important component of the persistent virus reservoir under antiretroviral therapy (9). The chronic expansion of T_{FH} in the case of HIV/SIV infection with persistent virus replication may be

*Emory Vaccine Center, Yerkes National Primate Research Center, Emory University, Atlanta, GA 30329; [†]Departamento de Investigación en Enfermedades Infecciosas, Instituto Nacional de Enfermedades Respiratorias, “Ismael Cosío Villegas,” Tlalpan, Sección XVI, 14080 City of Mexico Federal District, Mexico; and [‡]Department of Pediatrics, Emory University School of Medicine, Atlanta, GA 30329

Received for publication October 24, 2014. Accepted for publication July 13, 2015.

This work was supported by National Institutes of Health Grants U19 AI096187 and RR000165/OD011132 (to the Yerkes National Primate Research Center), and P30 AI050409 (to the Emory Center for AIDS Research).

The RNA sequencing data presented in this article have been submitted to the Gene Expression Omnibus (<http://www.ncbi.nlm.nih.gov/geo/query/acc.cgi?acc=GSE69756>) under accession number GSE69756.

Address correspondence and reprint requests to Dr. Guido Silvestri, Division of Microbiology and Immunology, Yerkes National Primate Research Center, Department of Pathology and Laboratory Medicine, Emory University School of Medicine, 924 Gatewood Road, Atlanta, GA 30329. E-mail address: gsilvest@emory.edu

The online version of this article contains supplemental material.

Abbreviations used in this article: bnAb, broadly neutralizing Ab; GC, germinal center; MFI, mean fluorescence intensity; MVA, modified vaccinia Ankara; RM, rhesus macaque; RNA-Seq, RNA sequencing; T_{FH} , T follicular helper cell; T_{FR} , T follicular regulatory cell; T_{REG} , regulatory T cell.

Copyright © 2015 by The American Association of Immunologists, Inc. 0022-1767/15/\$25.00

a direct result of antigenic persistence. As expected, HIV/SIV-associated expansion of T_{FH} is associated with dysregulation of B cell responses with ineffective memory cell formation and hypergammaglobulinemia (10, 11). Whether and to what extent this T_{FH} expansion is also related to a deficit in the physiological regulation of specific T_{FH} immune response within the lymph nodes remains unknown. However, this possibility would be consistent with the well-known observation that the chronic phase of pathogenic HIV/SIV infections is associated with a state of generalized immune activation that is resistant to the normal mechanisms of immune regulation.

Under normal circumstances, regulation of T_{FH} function is mediated, at least in part, by a recently described subset of $CD4^+$ T cells termed T follicular regulatory cells (T_{FR}). T_{FR} are thought to develop from thymic-derived regulatory T cells (T_{REG}) that express lineage-associated markers such as FOXP3, CD25, and low levels of CD127. These T_{FR} migrate into the follicles of lymph nodes by virtue of their expression of CXCR5 (and downmodulation of CCR7) and, similarly to T_{FH} , express high levels of Bcl-6 and PD1 (12, 13). Notably, the role of T_{FR} in the immunopathogenesis of HIV/SIV infections is currently unknown, both in terms of ability to negatively regulate HIV-specific B cell responses (including, potentially, the production of bnAbs) and to suppress local virus-induced immune activation. Indeed, none of the previous reports on T_{FH} dynamics in the context of SIV or HIV infection have distinguished between cells that either do or do not coexpress T_{REG} -associated markers. Thus, the T_{FR} subset within the broader $CXCR5^+Bcl-6^+PD1^+$ is not fully characterized in the setting of HIV/SIV infection.

In this study, we described and characterized phenotypically, histologically, and genomically the T_{FR} population that is found within the GCs of rhesus macaques (RM) and express markers associated with both T_{FH} and T_{REG} . The hypothesis that T_{FR} play a suppressive role in vivo is supported by the observation that their frequency is inversely correlated with both the levels of T_{FH} and GC B cells and the percentage of proliferating $CD4^+$ T cells. In the setting of SIV infection, we found that T_{FR} show a slow in vivo proliferative response after the initial infection and exhibit only a small increase in their frequency within the total $CD4^+$ T cell pool during the chronic phase. In conjunction with the large expansion of T_{FH} observed post SIV infection, this phenomenon leads to a significantly decreased T_{FR}/T_{FH} ratio in the lymph nodes of chronically SIV-infected RM. These data suggest that, during SIV infection, a lack of T_{FR} expansion may allow for a progressive accumulation of T_{FH} cells in the lymph nodes of chronically infected RM, thus indirectly contributing to the aberrant immune activation that characterizes this pathogenic infection.

Materials and Methods

Animals

This study involved a total of 40 Indian origin female RM divided as follows: 1) 10 healthy, unvaccinated, and SIV-uninfected RM; 2) 10 healthy, SIV-immunized, but SIV-uninfected RM; 3) 11 unvaccinated SIV-infected animals; and 4) 9 vaccinated and SIV-infected RM. Animals were vaccinated with a SIVmac239 Gag-, Pol-, and Env-expressing DNA vaccine with inactivating mutations in proteases, half of which also coexpressed GM-CSF. These were followed by two boosts of a SIVmac239 Gag-, Pol-, and Env-expressing modified vaccinia Ankara (MVA) vaccine as described previously (14). All infections were a result of SIVsmE660 intravaginal challenge at 2.06×10^4 50% tissue culture infective dose grown in RM PBMCs. Lymph node biopsies were collected for measurement of a number of immunological parameters at day -35 preinfection and days 14 and 168 postinfection (i.e., acute and chronic phase, respectively). Spleen and lymph nodes were collected at necropsies performed at 6 mo postinfection. All animals were housed at Yerkes National Primate Center at Emory University and were cared for in accordance with National Institutes of Health guidelines and following protocols approved by the Institutional Animal Care and Use Committee.

Tissue processing

Lymphocytes were isolated from freshly obtained lymph node and spleens by passing homogenized tissue through a 70- μ m cell strainer and lysing blood cells with ACK lysis buffer. Tissue collection and processing was performed as previously described (15). Cells to be later used for sorting were cryopreserved at -80°C in FBS media containing 10% DMSO.

Immunophenotyping and flow cytometry

Multicolor flow-cytometric analysis was performed on mononuclear cells isolated from blood and lymph nodes according to standard procedures using mAbs directed against RM markers and human markers that also cross-react with the same markers in RM. For optimum staining of intracellular markers, permeabilization of cells using the eBioscience FOXP3-permeabilization buffer was performed as recommended by the manufacturers. Predetermined optimal concentrations of the following Abs and reagents were used: CD3-Alexa 700 (clone SP34-2), CD4-allophycocyanin-Cy7 (clone OKT-4), Bcl-6-PE-Texas Red (clone K112-91), Ki67-FITC (clone B56), CCR5-PE (clone 3A9), and CTLA4-BV421 (clone BNI3) from BD; CXCR5-PerCP eFlour 710 (clone MU5BEE), PD1-PeCy7 (clone J105), and CD127-PeCy5 (clone eBio-RDR5) from eBioscience; and CD20-BV650 or PE-CF594 (clone 2H7), CD25-BV711 (clone BC96), Helios-FITC (clone 22F6), and FOXP3-allophycocyanin (clone 150D) from Biolegend; and Live/Dead Fixable Aqua from Invitrogen. Flow-cytometric data were acquired using LSRII flow cytometer using BD's FACSDiva software. Acquired data were analyzed using Flow Jo version 9.3.2 following the gating strategy described in Fig. 1. Further analyses were performed using PRISM (GraphPad) and Excel (Microsoft Office 2011) software.

Cell sorting

Cryopreserved cells were thawed in a 37°C water bath and rested overnight for 8–10 h and then stained for sorting. Splenocytes from five SIV-uninfected and unvaccinated RM, as well as five unvaccinated SIV-infected animals were used for sorting of T_{FH} , T_{FR} , and T_{REG} . Cell populations were sorted using FACSARIA II flow cytometer. Cells were first gated based on light scatter followed by positive gating on cells negative for Live/Dead Fixable Aqua and positive for CD3 and CD4. After collecting bulk $CD4^+$ cells the following three populations were collected: T_{FR} ($CXCR5^+PD1^{hi}CD127^-CD25^+$), T_{FH} ($CXCR5^+PD1^{hi}CD127^{+/-}CD25^-$), and T_{REG} ($CXCR5^{+/-}PD1^{lo/int}CD127^-CD25^+$).

Immunohistochemistry and confocal microscopy

Immunohistochemistry was performed on 5- μ m tissue sections mounted on glass slides, which were deparaffinized and rehydrated with double- dH_2O . Ag retrieval was performed in $1 \times$ Dako Target Retrieval Solution (pH 6.0) in a pressure cooker heating slides to 122°C for 30 s. Slides were then rinsed in ddH_2O and incubated for 10 min using Dako Protein block. Slides were then incubated with rabbit anti-CD4 (1:200), mouse anti-FOXP3 (1:100), and goat anti-PD1 (1:500) for 1 h at room temperature. Next, slides were washed in TBS with 0.05% Tween 20. Slides were then incubated for an hour in the dark with secondary Ab mixture containing donkey anti-rabbit Alexa 488 (1:500), donkey anti-mouse Alexa 594 (1:500), and donkey anti-goat Alexa 647 (1:500). After washing in TBS with 0.05% Tween 20, Prolong Gold with DAPI was applied to all the slides. Confocal microscope images were obtained using Olympus FV10i Confocal Microscope with CellSens 1.9 Digital Imaging software.

Quantitative PCR for SIV gag DNA

Cell-associated viral DNA was measured in sorted cell populations from RM lymph nodes by RT-PCR as previously described (16–18).

RNA-Seq library preparation

Total RNA was prepared using the QIAGEN RNeasy Micro Kit. Libraries were generated using the Clontech SMARTer HV kit, barcoding, and sequencing primers were added using Nextera XT DNA kit. Libraries were validated by microelectrophoresis, quantified, pooled, and clustered on Illumina TruSeq v3 flow cell. Clustered flow cell was sequenced on an Illumina HiSeq 1000 in 100-base single-read reactions.

RNA-sequencing data analysis

RNA sequencing (RNA-Seq) data were submitted to the Gene Expression Omnibus repository at the National Center for Biotechnology Information. RNA-Seq data were aligned to a provisional assembly of Indian *Macaca mulatta* (MaSuRCA rhesus assembly v.7_20130927) using STAR version 2.3.0e (19, 20). Transcripts were annotated using the provisional UNMC

annotation v7.6. Transcript assembly, abundance estimates, and differential expression analysis were performed using Cufflinks v2.1.1 and Cuffdiff (21). All samples had read counts >12,000,000 and unique mapping percentages in the range of 63–76%; no samples were excluded from the analysis for technical issues. Differentially expressed genes were defined by pairwise comparison of each phenotype. Differential gene lists were uploaded to Ingenuity Pathway Analysis software (v1.0 Ingenuity Systems, <http://www.ingenuity.com>) and pathways with significant enrichment by Fisher's exact test and the Benjamini-Hochberg multiple testing correction. Heat maps and other visualization were generated using Partek Genomics Suite v6.6. RNA-Seq data are publically available at the Gene Expression Omnibus repositories (accession number: GSE69756, <http://www.ncbi.nlm.nih.gov/geo/query/acc.cgi?acc=GSE69756>).

RT-PCR validation of RNA-sequencing data

Total RNA was prepared using the QIAGEN RNeasy Micro Kit from sorted T_{FR} , T_{FH} , and T_{REG} . RNA quantity was measured using Nanodrop analysis and reverse transcribed as previously described for RNA sequencing. Finally, 0.1 μ l cDNA was used for real-time SYBR green PCR analysis using an ABI 7900 HT real-time PCR instrument (Applied Biosystems). Primer sequences for PCR were GAPDH: forward (Fwd) 5'-GCACCACCAACTGCTTAG-CAC-3', reverse (Rev) 5'-TCTTCTGGGTGGCAGTGATG-3'; IL-2RA: Fwd 5'-GGCTTCATTTTCCACGGT-3', Rev 5'-GCAGCTGGCGGACCAA-3'; IL-6R: Fwd 5'-TTCGGCCGGACTGTTCTG-3', Rev 5'-GCACCCATCTCCGACG-3'; SLAMF6: Fwd 5'-TGG AAC ATC TCT TGC CTT CAT AG-3', Rev 5'-GTT GCT GAG TTT CAG GGA GTA G-3'; SAP/SH2D1A: Fwd 5'-CTCTGCAAGTATCCAGTTGAGAAG-3', Rev 5'-GGC TTT CAG GCA GAC ATC A-3'; XIAP: Fwd 5'-GAG GAA CCC TGC CAT GTA TAG-3', Rev 5'-GTG TAG TAG AGT CCA GCA CTT G-3'; PRDM1: Fwd 5'-TGT GGT ATT GTC GGG ACT TTG-3', Rev 5'-GCT TGA GAT TGC TCT GTG TTT G-3'; CCL20: Fwd 5'-GCA ACT TTG ACT GCT GTC TTC-3', Rev 5'-CAG CAT TGATGT CAC AGG TTT C-3'; PD1: Fwd 5'-TCCTTGGCCACTGGTGTTTC-3', Rev 5'-CTTCTCTGAGG-GAAGAGC-3'; IL-10: Fwd 5'-AAGACCTCAGGCTGAGGCT-3', Rev 5'-TCCACGGCCTTGCTCTTG-3'; IL-21: Fwd 5'-TGTGAATGACTT-GGACCCTGAA-3', Rev 5'-AAACAGGAAATAGCTGACCACTCA-3'. Relative RNA transcript levels were calculated normalized to primer efficiency and housekeeping gene RNA (GAPDH).

Statistical analyses

Except for RNA-Seq data, all statistical analyses were conducted using GraphPad Prism 5.0. Comparisons of mean fluorescence intensity (MFI) between cell populations in uninfected RM were made using Wilcoxon signed rank tests (Fig. 2). Mann-Whitney U tests were used to compare frequencies of populations in uninfected, acutely infected, and chronically infected RM (Figs. 4, 5). Spearman rank correlation tests were used to analyze all correlations (Fig. 6). All p values <0.05 were defined as significant.

Results

T_{FR} are distinct from T_{FH} and T_{REG} and can be found within lymph node GCs in RM

Recent studies of GC T_{FH} have defined these cells based on their surface expression of the chemokine receptor CXCR5 and very high levels of the coinhibitory receptor PD1 (10). However, a fraction of these canonically defined T_{FH} also express the lineage-specific T_{REG} marker FOXP3 and have been therefore defined as T_{FR} as proposed previously (22–24). In this article, we identified $CD4^+$ T_{FR} by flow cytometry by their coexpression of CXCR5, PD1, FOXP3, and CD25 within lymph nodes of uninfected RM. The gating strategy used to define T_{FH} , T_{FR} , and T_{REG} throughout this study is shown in Fig. 1A. Notably, the gating strategy for T_{REG} includes both CXCR5⁺ and CXCR5[−] cells. To confirm the presence of T_{FR} within GCs, we conducted an immunohistochemistry analysis. As shown in Fig. 1B, single cells with nuclear expression for FOXP3 and surface expression of PD1 were identified within GCs of uninfected RM. These T_{FR} can also be readily identified within GCs of SIV-infected RM (Fig. 1C). Interestingly, several bona fide T_{REG} , identified by their expression of FOXP3, but not PD1, are visible in the T cell zone just outside the GC (Fig. 1C). Presumably, some of these T_{REG} migrate into the GC and upregulate T_{FH} -like markers along their differentiation pathway to T_{FR} . Fig. 1B and 1C also show that, as

expected, non-FOXP3-expressing “true” T_{FH} are also seen within GCs of the same animals.

T_{FR} express markers of both T_{FH} and T_{REG} differentiation

We next performed a comprehensive examination of the T_{FR} phenotype in healthy, SIV-uninfected RM. As shown in Fig. 2, our analysis of relative MFIs for T_{FR} markers confirmed that T_{FR} express FOXP3 and CD25 at comparable levels with T_{REG} (Fig. 2A) and both CXCR5 and PD1 at comparable levels with T_{FH} (Fig. 2B). We next examined in T_{FR} the expression patterns of a series of markers (i.e., CD127, CTLA4, Bcl-6, and Helios) that have been linked to either T_{FH} or T_{REG} phenotype and function (1, 25). CD127, the IL-7R α -chain, is expressed at low levels on T_{REG} in humans (26–28). As expected, we found that T_{FR} express CD127 at lower levels than the bulk of $CD4^+$ T cells, and similar or even lower levels than those observed in T_{REG} and T_{FH} (Fig. 2C). CTLA4 is a key negative T cell regulator that is constitutively expressed on T_{REG} and, upon ligation, induces downmodulation of cytokine production and inhibition of cell cycle progression (25). Consistent with previous reports in murine models (12), we observed that T_{FR} express CTLA4 at a higher frequency and MFI than both T_{REG} and T_{FH} cell populations (Fig. 2D). This is consistent with a putative role of T_{FR} as negative regulators of GC responses. Helios is a transcription factor expressed in thymus-derived natural T_{REG} (29). As shown in Fig. 2F, T_{FR} express Helios at levels that are even higher than those observed in T_{REG} in terms of both frequency of positive cells and MFI, thus suggesting that T_{FR} originate from natural T_{REG} in RM, as well as in mice.

Transcriptome analysis of T_{FR} reveals a distinct but overlapping transcriptional profile compared with T_{FH} and T_{REG}

To further define the functional features of T_{FR} in RM, we next examined the transcriptional profiles of T_{FH} , T_{FR} , and T_{REG} using RNA-Seq by Illumina technology. Splenocytes from five healthy, SIV-uninfected, and unvaccinated RM were sorted into “bulk” $CD3^+$ $CD4^+$ T cells, T_{REG} , T_{FH} , and T_{FR} based on the following phenotypic markers: T_{FR} (CXCR5⁺PD1^{hi}CD127[−]CD25⁺), T_{FH} (CXCR5⁺PD1^{hi}CD127^{+/−}CD25[−]), and T_{REG} (CXCR5^{+/−}PD1^{lo/int}CD127[−]CD25⁺). In mice, T_{FR} are derived from thymic T_{REG} precursors and acquire homing markers that allow them to traffic to GCs, while maintaining a transcriptome and suppressive function that most closely resembles T_{REG} (12, 13). To examine the transcriptional profile of T_{FR} relative to T_{REG} and T_{FH} in healthy, SIV-uninfected RM, we first performed principal component analysis on a subset of the most highly expressed transcripts detected in T_{FH} , T_{REG} , and T_{FR} (Fig. 3A). The transcriptomes of each subset were clearly distinct and grouped by subset, with T_{REG} displaying the highest degree of intrasubset variability, and T_{FH} and T_{FR} subsets being more tightly distributed. We next compared the expression of several canonical T_{FH} and T_{REG} transcripts between the three subsets. As shown in Fig. 3B–D, T_{FH} - and T_{REG} -related genes showed expression patterns that behaved as predicted with genes such as IL-10 expressed in T_{FR} and T_{REG} but absent in T_{FH} . Importantly, RNA-Seq data confirmed that T_{FR} share expression of T_{REG} signature transcripts such as FOXP3, GZMB, PRDM1, and IL-2RA (Fig. 3). However, we found that several other T_{REG} -specific transcripts were expressed at lower levels in T_{FR} than in T_{REG} , including TRAF6, CD74, CCL20, and IL-1R1. Similar to previous studies in mice, T_{FR} also showed elevated expression of the prototypical T_{FH} genes CXCR5, PD1/PDCD1, BCL-6, CXCL13, and ICOS. In fact, T_{FR} demonstrated a peculiarly high expression of the T_{FH} - and T_{REG} -specific genes Bcl-6 and FOXP3, respectively. Interestingly, for several genes (SH2D1A/SAP, IL-21, CXCR5, IL-10), gene expression was higher

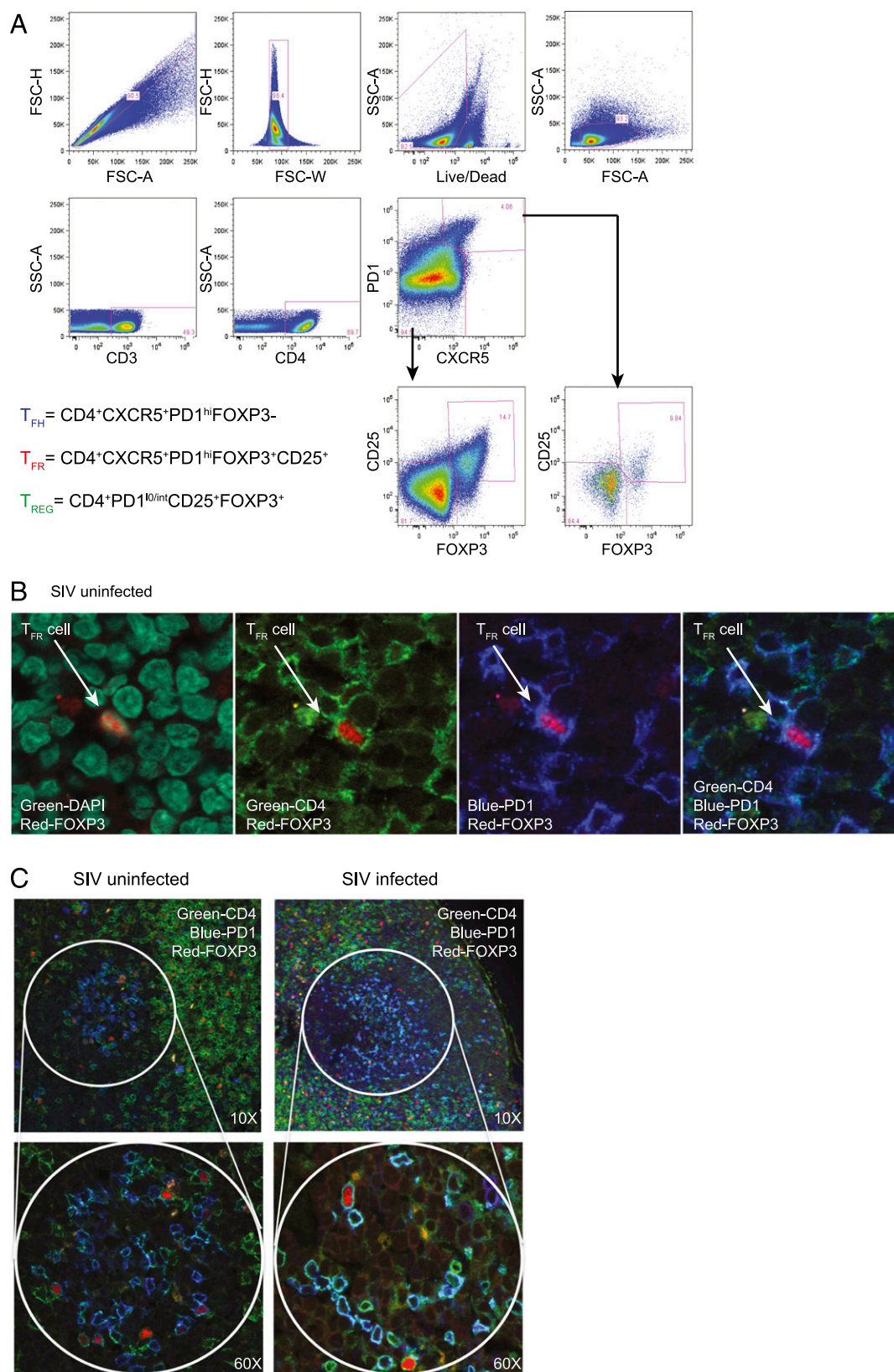


FIGURE 1. T_{FR} can be defined by flow cytometry and identified by confocal microscopy within the GCs of RM. **(A)** Representative flow-cytometry plot of lymphocytes from lymph nodes of untreated, uninfected RM showing the gating strategy used to define T_{FR} , T_{FH} , and T_{REG} populations. **(B)** Representative confocal microscope image showing a single T_{FR} within the lymph node of an uninfected RM. The *first image* shows staining for DAPI (green) and FOXP3 (red), the *second image* shows the same section with CD4 (green) and FOXP3 (red), the *third image* PD1 (blue) and FOXP3 (red), and the *last image* CD4 (green), PD1 (blue), and FOXP3 (red). Original magnification $\times 120$. **(C)** Representative images of lymph node biopsies from SIV-uninfected and acutely infected RM showing cells stained with CD4 (green), FOXP3 (red), and PD1 (blue) within the GC regions.

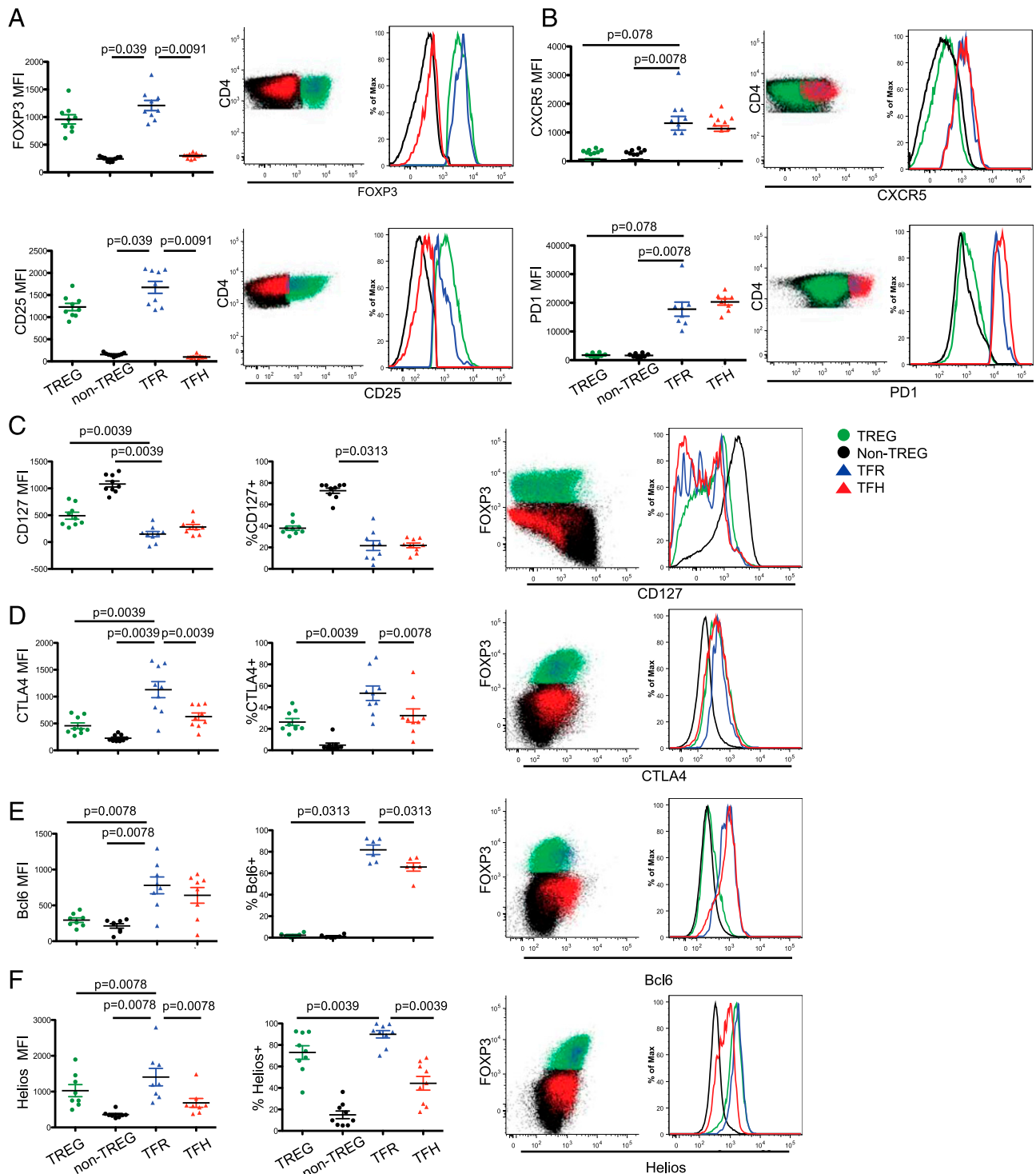


FIGURE 2. T_{FR} share immunophenotypic features of both T_{FH} and T_{REG} populations. MFI, percent positive, representative flow-cytometry plots, and histograms (A–F) for expression of various immunophenotypic markers (i.e., FOXP3, CD25, CXCR5, PD-1, CD127, CTLA4, Bcl-6, and Helios) among T_{REG}, non-T_{REG}, T_{FR}, and T_{FH} populations from lymph node of healthy, unvaccinated, and uninfected RM. Non-T_{REG} are defined as all CD4⁺CD25[−]FOXP3[−] T cells. Significance was determined by Wilcoxon signed rank tests.

in T_{FR} than either T_{REG} or T_{FH}, thus suggesting that the CD25⁺CXCR5⁺PD1^{hi} phenotype may represent a more transcriptionally active population than classical T_{REG} or T_{FH}. This latter set of RNA-Seq data provides strong evidence that T_{FR} are indeed a distinct cell subset and that the somewhat hybrid transcriptional profile of T_{FR} is not simply due to the sample being a mixture of T_{REG} and T_{FH}. Notably, elevated expression of IL-10 in T_{FR} compared with T_{REG} has been previously reported in murine studies (13).

To then compare the profile of gene expression between T_{FR} with T_{REG} and T_{FH} subsets without using any a priori information, we defined T_{FH} and T_{REG} expression signatures by statistically contrasting RNA-Seq data from T_{FH} and T_{REG} with bulk CD4⁺ T cells. After exclusion of transcripts that had zero expression in any of the populations, a total of 88 genes made up the combined T_{FH} and T_{REG} signature of which 12 genes were T_{REG} related. Many, but not all, canonical T_{REG} and T_{FH} genes were also identified as significantly

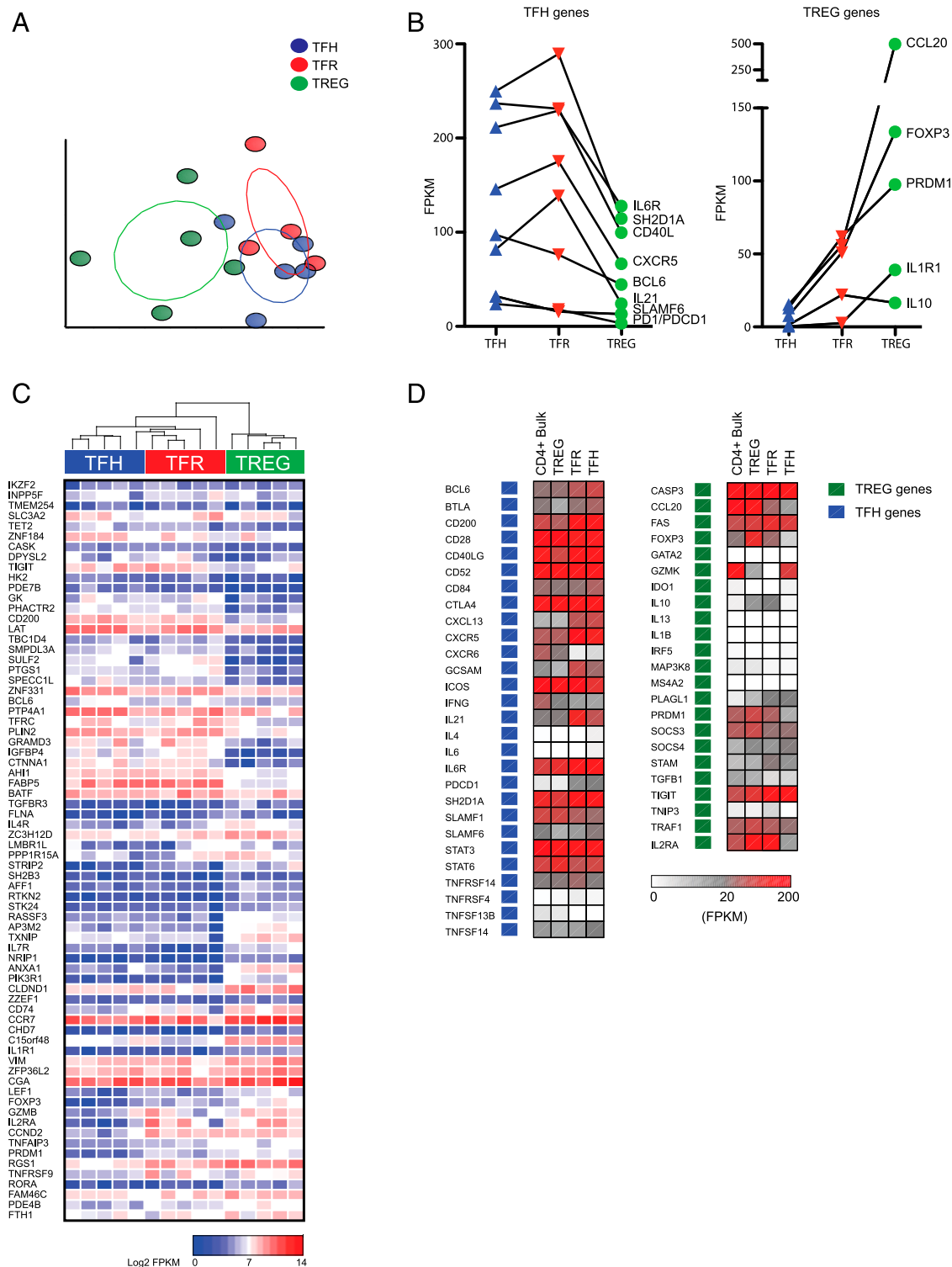


FIGURE 3. RNA expression patterns confirm that T_{FR} share T_{FH} - and T_{REG} -like phenotype. **(A)** Principal components analysis of RNA transcripts from five healthy, SIV-uninfected RM. Each circle represents the transcriptome of a sorted population of T_{FH} (blue), T_{REG} (green), or T_{FR} (red) from a single animal. **(B)** Expression in fragments per kilobase of transcript per million mapped reads (FPKM) of select T_{FH} and T_{REG} genes in sorted populations from uninfected RM. **(C)** Heat map of log 2 transformed gene expression of transcripts in FPKM. Transcripts represent T_{FH} and T_{REG} signature genes. The T_{FH} gene signature was defined as transcripts that were significantly differentially expressed in sorted T_{FH} compared with bulk $CD4^+$ T cells. T_{REG} gene signature was defined as genes that were significantly differentially expressed in sorted T_{REG} compared with bulk $CD4^+$ T cells. **(D)** Expression pattern of key T_{FH} and T_{REG} genes in sorted bulk $CD4^+$ T cell, T_{FH} , T_{FR} , and T_{REG} populations.

upregulated compared with bulk $CD4^+$ T cells. The lack of statistical significance for some prototypical transcripts is likely due to the presence T_{REG} and T_{FH} subsets within the bulk $CD4^+$ population used as a comparator sample. Nevertheless, we found that T_{FR}

show similar levels of expression of T_{FH} signature genes such as Bcl-6, TIGIT, CD200, LATm, and BATF (Fig. 3C). T_{FR} cells also express mRNA for key T_{FH} -related genes that are important for B cell help, including IL-21, SH2D1A, CD40L, and CD84. One

notable difference between our data in RM and previously published mouse studies is that we observed high expression of IL-21 in T_{FR} , suggesting that these cells have acquired some specific genomic and functional features in primates. As shown in Supplemental Fig. 2A–C, the expression patterns of IL-21, SH2D1A, SLAMF6, PD1, IL-6R, CCL20, IL-2RA, IL-10, PRDM1, and XIAP were confirmed by RT-PCR quantification. In addition, levels of protein expression of IL-21 by T_{FR} , T_{FH} , and T_{REG} were also measured by flow cytometry and further confirmed the pattern observed by RNA sequencing and RT-PCR (Supplemental Fig. 2D).

SIV infection is associated with a decrease in the T_{FR}/T_{FH} ratio

The dynamics of T_{FR} in the setting of HIV or SIV infection have not been previously investigated; in fact, all published studies of T_{FH} dynamics during HIV/SIV infection used a definition of these cells that included T_{FR} as well. To study the kinetics of T_{FR} , T_{FH} , and T_{REG} post SIV infection of RM, we measured the frequency of these cells within the lymph nodes preinfection, 2 wk postinfection, and 6 mo postinfection with SIVsmE660. The RM included in these kinetics analyses included both unvaccinated and animals that were challenged after immunization with a SIVmac239 Gag-, Pol-, and Env-expressing DNA vaccine (with or without GM-CSF) followed by two boosts of a SIV239 Gag-, Pol-, and Env-expressing MVA vaccine. As previously reported, we found a significant increase ($p < 0.0001$) in frequency of T_{FH} at 24 wk postinfection (Fig. 4A). Interestingly, the frequency of T_{FR} measured as percent of total $CD4^+$ T cells also showed a significant ($p = 0.0001$) increase during chronic SIV infection (Fig. 4A). However, when the frequency of T_{FR} is measured as percentage of total T_{FH} , we found that the T_{FR} decrease significantly at both the acute ($p = 0.0385$) and the chronic ($p = 0.0016$) stages of SIV infection (Fig. 4B). Accordingly, the overall ratio of T_{FR} to T_{FH} also decreased significantly ($p = 0.0018$) at the week 24 postinfection time point as compared with baseline (Fig. 4C). The increase of both T_{FH} and T_{FR} as a percent of $CD4^+$ T cells postinfection is likely the result of proliferation driven by Ag

persistence and virus-mediated depletion of other $CD4^+$ T cell subsets. However, the relative decrease in the frequency of T_{FR} when measured as percentage of T_{FH} suggests that the low frequency of these regulatory cells might contribute to the expansion and accumulation of T_{FH} in chronically SIV-infected RM. Notably, we found no significant changes in T_{REG} frequencies after SIV infection within the lymph nodes. To better define the kinetics of T_{FH} and T_{FR} during SIV infection, we next measured the level of cell proliferation using the well-established marker Ki67. We observed that T_{FH} show a significant increase in proliferating cells during the acute ($p < 0.0001$) and chronic ($p = 0.0001$) phases of infection (Fig. 4D). T_{FR} have a similar pattern of proliferation, with a significant increase in proliferating cells during the acute ($p < 0.0001$) and chronic ($p = 0.0376$) phases of infection (Fig. 4D). In contrast, the level of Ki67 expression in T_{REG} remains relatively low throughout our analysis with a small, significant increase ($p = 0.0141$) during the chronic phase of infection (Fig. 4D).

Similar levels of SIV infection of T_{FR} as compared with T_{FH} and T_{REG} despite higher CCR5 expression

Several studies have shown that, during HIV and SIV infection, T_{FH} are highly infected with the virus despite their relative increase within the total $CD4^+$ T cell pool (9). Although the actual in vivo life span of T_{FH} , either infected or uninfected, remains unknown in the setting of HIV/SIV infection, the presence of a notable fraction of these cells expressing the proliferation marker Ki67 suggests that their number could be maintained through continual replenishing from precursors located outside the GC. To measure the level of direct SIV infection of T_{FR} , T_{FH} , and T_{REG} , we sorted these subpopulations from the lymph nodes of a subset of our studied animals and quantified the levels of total cell-associated SIV-DNA by RT-PCR. This analysis revealed that T_{FH} , T_{FR} , and T_{REG} derived from chronically SIV-infected RM all harbor comparably high levels of cell-associated viral DNA (Fig. 5A). Interestingly, the levels of SIV infection were similarly high between T_{FR} and T_{FH} even though the

FIGURE 4. Kinetics of T_{FR} , T_{FH} , and T_{REG} after SIV infection. **(A)** Frequency of T_{FH} , T_{FR} , and T_{REG} as percentage of the total $CD4^+$ T cell population within lymph nodes of uninfected, acutely (week 2) SIV-infected, and chronically (week 24) SIV-infected RM. **(B)** Frequency of T_{FR} as a percent of T_{FH} within the lymph nodes of the same animals. **(C)** Ratio of frequencies of T_{FR} to the frequency of T_{FH} (both calculated as a percent of the total $CD4^+$ T cell population). **(D)** Percent of proliferating, Ki67 $^+$, T_{FH} , T_{FR} , and T_{REG} within the lymph nodes of uninfected, acutely SIV-infected, and chronically SIV-infected RM. Statistical analyses were performed using Mann–Whitney U tests.

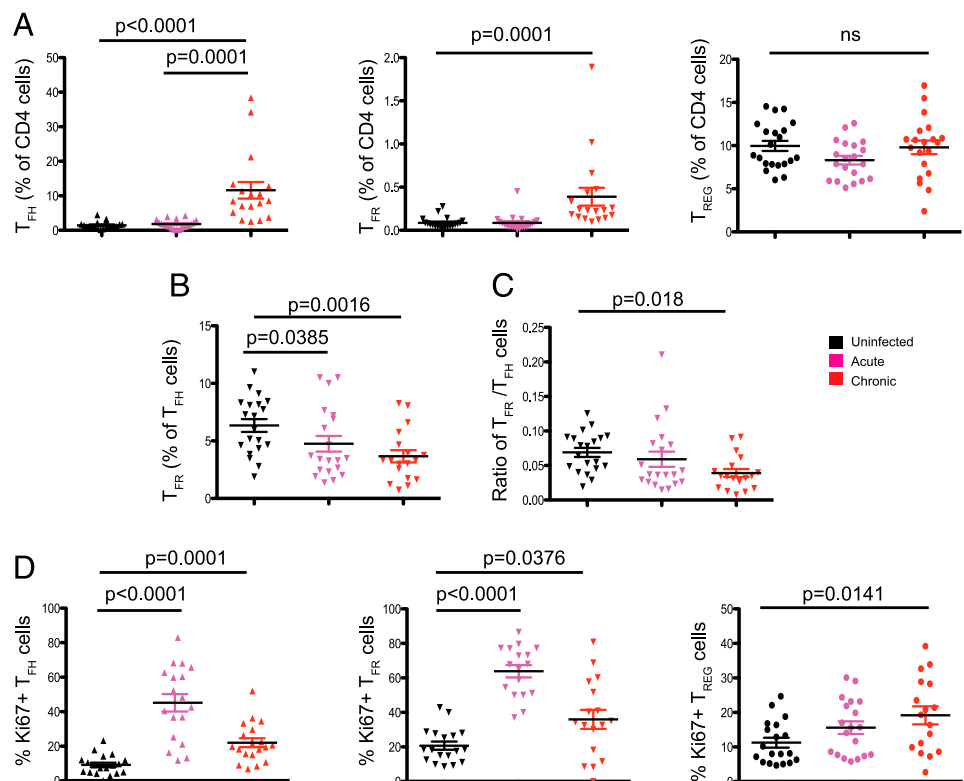
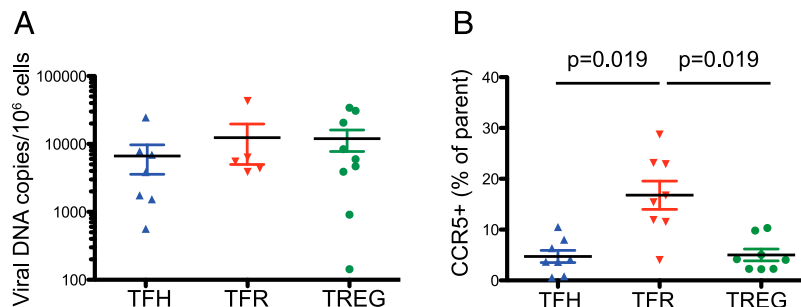


FIGURE 5. Comparable levels of SIV infection in T_{FH} , T_{FR} , and T_{REG} isolated from the spleen of chronically SIV-infected RM. **(A)** Viral DNA copies per million sorted T_{FH} , T_{FR} , and T_{REG} from spleens of unvaccinated, chronically SIV-infected RM. **(B)** Percent of CCR5-expressing cells among T_{FH} , T_{FR} , and T_{REG} in unvaccinated SIV-infected RM. Statistical analyses were performed using Mann–Whitney U tests.



surface expression levels of the main SIV coreceptor CCR5 were significantly higher in T_{FR} as compared with T_{FH} (Fig. 5B).

Frequency of T_{FR} is negatively correlated with the number and proliferation of both T_{FH} and GC B cells

To further examine the relationship between T_{FR} and T_{FH} and GC B cells, we next performed a set of correlation analyses in the RM included in this study. We observed that, in healthy uninfected RM, the frequency of T_{FR} (as fraction of the total T_{FH} pool) is negatively correlated with the percentages of T_{FH} (as fraction of total CD4⁺ T cells) and GC B cells (as fraction of total B cells) (Fig. 6A). In addition, we found that, in the same animals, the frequency of T_{FR} (as fraction of T_{FH}) is negatively correlated with the level of CD4⁺ T cell proliferation as measured by Ki67 expression (Fig. 6A).

We next performed the same correlation analyses in our cohort of SIV-infected RM. The SIV-infected RM included in these regression analyses included both unvaccinated and animals that were challenged after immunization with an SIVmac239 Gag-, Pol-, and Env-expressing DNA vaccine (with or without GM-CSF) followed by two boosts of an SIV239 Gag-, Pol-, and Env-expressing MVA vaccine. In the SIV-infected RM, similar to what was observed in uninfected animals, the frequency of T_{FR} (as fraction of T_{FH}) is negatively

correlated with the percentages of both T_{FH} and GC B cells (Fig. 6B). However, the negative correlation between frequency of T_{FR} (as fraction of T_{FH}) and the level of CD4⁺ T cell proliferation as measured by Ki67 expression is not seen in SIV-infected RM (Fig. 6B). The negative correlation between T_{FR} cells (as a frequency of T_{FH} cells) and both T_{FH} and GC B cell frequencies is consistent with the hypothesis that T_{FR} cells play a role in regulating T_{FH} and GC responses under normal circumstances and in the setting of chronic SIV infection.

Comparative analysis of the T_{FR} transcriptome in SIV-infected and uninfected RM

To further define the effect of SIV infection on T_{FR} , we next compared the transcription profiles of T_{FR} that were isolated from unvaccinated, chronically SIV-infected and uninfected RM (Fig. 7). We performed RNA-Seq analysis, and transcripts that were significantly differentially expressed in T_{FR} sorted from SIV-infected versus uninfected RM were analyzed by Ingenuity Pathway Analysis. Unsurprisingly, a large proportion of genes induced during SIV infection in T_{FR} (CD3G, FOS, CD4, ZAP70, PIK3CD, STAT3) were components of T cell proliferation, activation of T cell effector function, and costimulatory activation (data not shown).

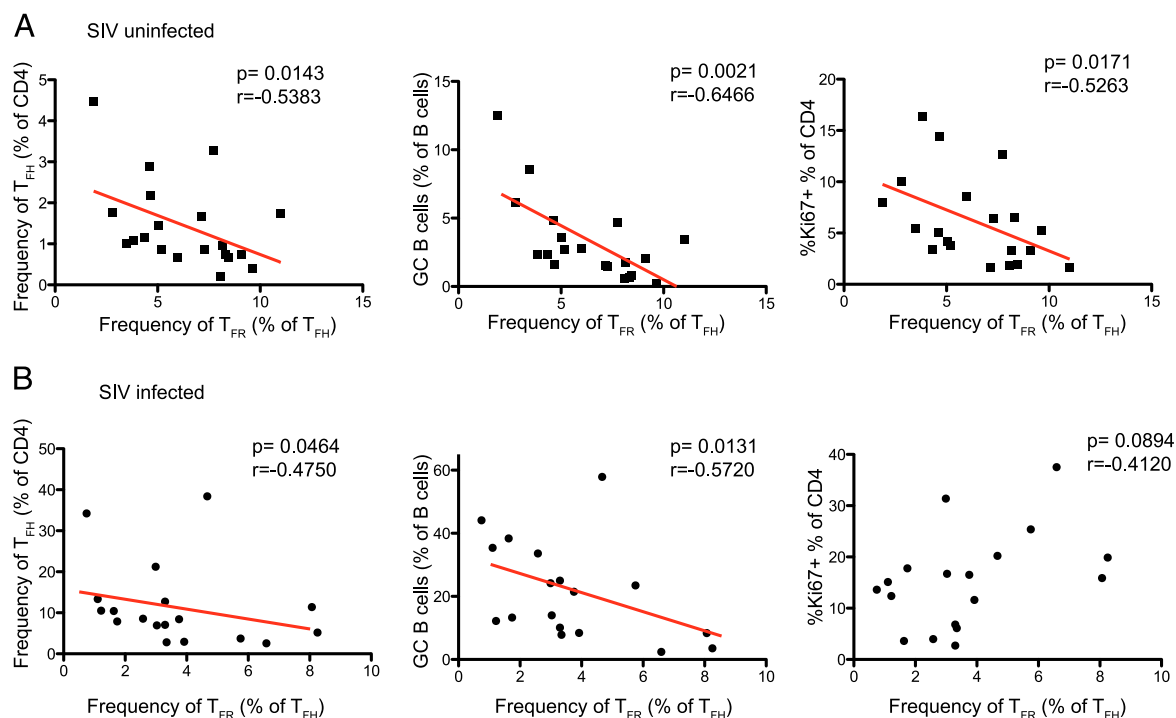


FIGURE 6. T_{FR} frequencies negatively correlate with T_{FH} and GC B cell frequencies in the lymph nodes of RM. Correlations between the frequencies of T_{FR} (calculated as frequency of T_{FH}) and the frequencies of T_{FH} calculated as percent of total CD4⁺ T cells (*left panels*) and GC B cells calculated as percent of total B cells (*center panels*) and proliferating (i.e., Ki67⁺) CD4⁺ T cells (*right panels*) within the lymph nodes of SIV-uninfected (**A**) and chronically SIV-infected (**B**) RM. Statistical analyses were performed using Spearman rank correlation tests.

B

T_{FH} cells

Gene	Log2 fold change (approx.)
CXCR5	0.8
BCL6	-0.5
IL21	3.5
SH2D3A	0.0
ILAP	1.0
ICOS	-0.5
CD40L	-0.2
CD2	2.4
SLAMF1	0.4
CD27	-2.1
CTLA4	0.0
SLAMF5	-2.2
SLAMF7	2.1
OXCL13	2.8
CD28	-1.2
CD280	-0.3
CD286	1.3
BTUL44	0.3
LIGHT	0.4
IL21R	0.4
CD285	-1.2
IFNG	0.7
MVC	1.1
LOX	0.5
FLT3LG	0.0

T_{REG} cells

Gene	Log2 fold change (approx.)
FOXP3	-1.0
IKZF2	0.0
IL10	0.6
TGFB	0.8
CCL20	-2.5
SOCS2	-0.7
IL7R	1.8
IL2RA	-2.2
MGARP	-2.1
PRDM1	-0.8
GATA3	0.4
CASP3	-1.6
FOXP1	-0.2
IL2RB	-1.2
IL1R1	0.0

The enhanced T cell activation was consistent with our observation that T_{FR} cells express higher levels of the proliferation marker Ki67 compared with T_{REG} (Fig. 4D). We also observed that several genes implicated in pathways regulating apoptosis or cell-cycle control were perturbed in SIV-infected RM. Of particular interest was the observation that the proapoptotic gene FASLG was >100-fold induced, whereas the antiapoptotic regulator XIAP was significantly

The main findings of this study are the following: 1) T_{FR} show distinct yet overlapping phenotype as compared with T_{FH} and T_{REG} based on a combination of flow cytometric, histological, and transcriptional analyses; 2) in healthy, SIV-uninfected RM, the frequencies of T_{FR} are negatively correlated with the levels of both T_{FH} and GC B cells; 3) post SIV infection, the T_{FR}/T_{FH} ratio is reduced; and 4) T_{FR} sorted from SIV-infected RM harbor comparable levels of cell-associated viral DNA as compared with T_{FH} and T_{REG} . Collectively, these data indicate that although T_{FR} closely resemble T_{FH} in several aspects, they are also clearly distinguishable from

this cell subset in terms of both their immunophenotype and transcriptional profile. It is therefore important that, in future studies of T_{FH} , a distinction be made between T_{FR} and true “non- T_{FR} ” T_{FH} to fully take into account the complexity of the different $CD4^+$ T cell subsets that are present in the GC.

The observation that T_{FR} express proteins typically expressed by T_{FH} , such as CD40L, as well as proteins typically expressed by T_{REG} , like IL-10 and CTLA4, is consistent with studies in mice showing that T_{FR} are thymic-derived T_{REG} that migrate into the follicle and, in a manner similar to T_{FH} , upregulate CXCR5, Bcl-6, and PD1 in a B cell-dependent manner (24). The production of IL-21 by T_{FR} is an intriguing new finding and suggests that T_{FR} play a more complex role in RMs than has been described in mice. In addition, principal component analysis suggests that the transcriptional profile of T_{FR} tends to be more similar to T_{FH} than T_{REG} . Further studies are required to fully investigate the functional role played by T_{FR} in RMs and, specifically, in the context of SIV infection. The finding that >90% of T_{FR} express Helios as measured by flow cytometry is also consistent with the natural T_{REG} origin of these cells. Importantly, these immunophenotypic and RNA-Seq data were complemented by histological analyses showing that T_{FR} are found within GCs of both uninfected and infected RM. Although $CD4^+FOXP3^+T_{REG}$ were found in abundance outside the GC, $CD4^+PD1^+T_{FH}$ and $CD4^+PD1^+FOXP3^+T_{FR}$ were both only seen within the GC. The hypothesis that T_{FR} play an immune-regulatory role in vivo is supported by the observation that their frequency is inversely correlated with the levels of both T_{FH} and GC B cells. These data are consistent with mouse studies indicating that: 1) T_{FR} suppress T_{FH} in vitro and prevent the outgrowth of non-Ag-specific B cells (13); and 2) T_{FR} may inhibit Ab production without an effect on T cell activation, thus indicating an ability to directly regulate B cells (32).

In the setting of in vivo SIV infection, we found that T_{FR} exhibited only a small increase in their frequency within the total $CD4^+$ T cell pool. In conjunction with the large expansion of T_{FH} that is consistently observed post SIV infection, the minor expansion of T_{FR} leads to a significantly decreased T_{FR}/T_{FH} ratio in the lymph nodes of chronically SIV-infected RM. We confirmed this trend in the ratio of T_{FR}/T_{FH} cells after SIV infection by quantifying the number of T_{FH} and T_{FR} cells by immunohistochemistry (Supplemental Table I). Although the present set of results does not allow us to determine whether and to what extent the kinetics of T_{FH} and T_{FR} during SIV infection are mechanistically linked, it is conceivable that the limited T_{FR} expansion facilitates progressive accumulation of T_{FH} in chronically SIV-infected RM, thus indirectly contributing to the aberrant immune activation that characterizes this pathogenic infection. In contrast, it is also possible that the strong proliferation of T_{FH} and associated increase in PD1 expression post SIV infection hampers the development or differentiation of T_{FR} as suggested previously (32).

Comparison of the transcriptional profiles of T_{FR} cells before and post SIV infection showed a significant upregulation of transcripts typically expressed by activated T_{REG} including FOSB, FABP5, USP2, and USP13 (data not shown) (33), thus suggesting that T_{FR} may be involved in the generalized immune activation associated with pathogenic SIV infection. Interestingly, we also observed a downregulation of several T_{FH} and T_{REG} signature genes as established by our own algorithm. This somewhat unexpected observation indicates that SIV infection has a complex effect on the in vivo phenotype and function of T_{FR} . A better understanding of the overall contribution of T_{FR} to the immunopathogenesis of AIDS, in terms of causing either the virus-associated B cell dysfunction or the changes in the lymph node architecture and function, will require further in vitro and in vivo investigation of the suppressive effect by these T_{FR} on the function of either T_{FH} or GC B cells.

Although $CD4^+$ T cells are the main target for HIV and SIV infection, substantial differences exist between various $CD4^+$ T cell subsets in terms of their relative levels of direct virus infection in vivo (34–36). In this study, we tested the possibility that the decrease in the T_{FR}/T_{FH} ratio observed during SIV infection of RM was associated with higher level of virus infection in T_{FR} as compared with T_{FH} . However, our comparative analysis of the cell-associated viral burdens in sorted T_{FR} , T_{FH} , and T_{REG} revealed similar levels of SIV-DNA in the three $CD4^+$ T cell subsets, even though T_{FR} exhibited higher levels of the SIV coreceptor CCR5 as compared with the other two subsets.

In summary, to our knowledge, the presented data provide the first comprehensive description of T_{FR} in healthy, uninfected RM, as well as the first examination of the kinetics of these cells in the setting of pathogenic SIV infection. These results support the hypothesis that these cells play an important immune-regulatory role in vivo, and that a relative decline of the T_{FR}/T_{FH} ratio may be involved in establishing a state of chronic immune activation in the B cell areas of lymph nodes during pathogenic HIV and SIV infection.

Acknowledgments

We thank Drs. Barbara Cervasi and Kiran Gill at the Flow Cytometry Core (Emory Vaccine Center) and Drs. Prachi Sharma and Deepa Kodandera at the Molecular Pathology Core Lab (Yerkes National Primate Research Center). We also thank the animal care and veterinary staff at the Yerkes National Primate Research Center.

Disclosures

The authors have no financial conflicts of interest.

References

- Pissani, F., and H. Streeck. 2014. Emerging concepts on T follicular helper cell dynamics in HIV infection. *Trends Immunol.* 35: 278–286.
- Corti, D., and A. Lanzavecchia. 2013. Broadly neutralizing antiviral antibodies. *Annu. Rev. Immunol.* 31: 705–742.
- Murphy, M. K., L. Yue, R. Pan, S. Boliari, A. Sethi, J. Tian, K. Pfafferot, E. Karita, S. A. Allen, E. Cormier, et al. 2013. Viral escape from neutralizing antibodies in early subtype A HIV-1 infection drives an increase in autologous neutralization breadth. *PLoS Pathog.* 9: e1003173.
- Crotty, S. 2011. Follicular helper CD4 T cells (TFH). *Annu. Rev. Immunol.* 29: 621–663.
- Pratama, A., and C. G. Vinuesa. 2014. Control of TFH cell numbers: why and how? *Immunol. Cell Biol.* 92: 40–48.
- Yang, X., J. Yang, Y. Chu, Y. Xue, D. Xuan, S. Zheng, and H. Zou. 2014. T follicular helper cells and regulatory B cells dynamics in systemic lupus erythematosus. *PLoS One* 9: e88441.
- Ma, C. S., and E. K. Deenick. 2014. Human T follicular helper (Tfh) cells and disease. *Immunol. Cell Biol.* 92: 64–71.
- Vinuesa, C. G. 2012. HIV and T follicular helper cells: a dangerous relationship. *J. Clin. Invest.* 122: 3059–3062.
- Perreau, M., A. L. Savoye, E. De Crignis, J. M. Corpataux, R. Cubas, E. K. Haddad, L. De Leval, C. Graziosi, and G. Pantaleo. 2013. Follicular helper T cells serve as the major CD4 T cell compartment for HIV-1 infection, replication, and production. *J. Exp. Med.* 210: 143–156.
- Lindqvist, M., J. van Lunzen, D. Z. Soghoian, B. D. Kuhl, S. Ranasinghe, G. Kranias, M. D. Flanders, S. Cutler, N. Yudanin, M. I. Muller, et al. 2012. Expansion of HIV-specific T follicular helper cells in chronic HIV infection. *J. Clin. Invest.* 122: 3271–3280.
- Petrovas, C., and R. A. Koup. 2014. T follicular helper cells and HIV/SIV-specific antibody responses. *Curr. Opin. HIV AIDS* 9: 235–241.
- Chung, Y., S. Tanaka, F. Chu, R. I. Nurieva, G. J. Martinez, S. Rawal, Y. H. Wang, H. Lim, J. M. Reynolds, X. H. Zhou, et al. 2011. Follicular regulatory T cells expressing Foxp3 and Bcl-6 suppress germinal center reactions. *Nat. Med.* 17: 983–988.
- Linterman, M. A., W. Pierson, S. K. Lee, A. Kallies, S. Kawamoto, T. F. Rayner, M. Srivastava, D. P. Divekar, L. Beaton, J. J. Hogan, et al. 2011. Foxp3+ follicular regulatory T cells control the germinal center response. *Nat. Med.* 17: 975–982.
- Lai, L., S. Kwa, P. A. Kozlowski, D. C. Montefiori, G. Ferrari, W. E. Johnson, V. Hirsch, F. Villinger, L. Chennareddi, P. L. Earl, et al. 2011. Prevention of infection by a granulocyte-macrophage colony-stimulating factor co-expressing DNA/modified vaccinia Ankara simian immunodeficiency virus vaccine. *J. Infect. Dis.* 204: 164–173.
- Ortiz, A. M., N. R. Klatt, B. Li, Y. Yi, B. Tabb, X. P. Hao, L. Sternberg, B. Lawson, P. M. Carnathan, E. M. Cramer, et al. 2011. Depletion of $CD4^+$ T cells abrogates post-peak decline of viremia in SIV-infected rhesus macaques. *J. Clin. Invest.* 121: 4433–4445.

16. Cartwright, E. K., C. S. McGary, B. Cervasi, L. Micci, B. Lawson, S. T. Elliott, R. G. Collman, S. E. Bosinger, M. Paiardini, T. H. Vanderford, et al. 2014. Divergent CD4+ T memory stem cell dynamics in pathogenic and nonpathogenic simian immunodeficiency virus infections. *J. Immunol.* 192: 4666–4673.
17. Vanderford, T. H., C. Slichter, K. A. Rogers, B. O. Lawson, R. Obaede, J. Else, F. Villinger, S. E. Bosinger, and G. Silvestri. 2012. Treatment of SIV-infected sooty mangabeys with a type-I IFN agonist results in decreased virus replication without inducing hyperimmune activation. *Blood* 119: 5750–5757.
18. Klatt, N. R., E. Shudo, A. M. Ortiz, J. C. Engram, M. Paiardini, B. Lawson, M. D. Miller, J. Else, I. Pandrea, J. D. Estes, et al. 2010. CD8+ lymphocytes control viral replication in SIVmac239-infected rhesus macaques without decreasing the lifespan of productively infected cells. *PLoS Pathog.* 6: e1000747.
19. Sandler, N. G., S. E. Bosinger, J. D. Estes, R. T. Zhu, G. K. Tharp, E. Boritz, D. Levin, S. Wijeyesinghe, K. N. Makamdop, G. Q. del Prete, et al. 2014. Type I interferon responses in rhesus macaques prevent SIV infection and slow disease progression. *Nature* 511: 601–605.
20. Dobin, A., C. A. Davis, F. Schlesinger, J. Drenkow, C. Zaleski, S. Jha, P. Batut, M. Chaisson, and T. R. Gingeras. 2013. STAR: ultrafast universal RNA-seq aligner. *Bioinformatics* 29: 15–21.
21. Trapnell, C., D. G. Hendrickson, M. Sauvageau, L. Goff, J. L. Rinn, and L. Pachter. 2013. Differential analysis of gene regulation at transcript resolution with RNA-seq. *Nat. Biotechnol.* 31: 46–53.
22. Vinuesa, C. G., and J. G. Cyster. 2011. How T cells earn the follicular rite of passage. *Immunity* 35: 671–680.
23. Alexander, C. M., L. T. Tygrett, A. W. Boyden, K. L. Wolniak, K. L. Legge, and T. J. Waldschmidt. 2011. T regulatory cells participate in the control of germinal centre reactions. *Immunology* 133: 452–468.
24. Wollenberg, I., A. Agua-Doce, A. Hernández, C. Almeida, V. G. Oliveira, J. Faro, and L. Graca. 2011. Regulation of the germinal center reaction by Foxp3 + follicular regulatory T cells. *J. Immunol.* 187: 4553–4560.
25. Wing, J. B., and S. Sakaguchi. 2014. Foxp3+ T(reg) cells in humoral immunity. *Int. Immunol.* 26: 61–69.
26. Liu, W., A. L. Putnam, Z. Xu-Yu, G. L. Szot, M. R. Lee, S. Zhu, P. A. Gottlieb, P. Kapranov, T. R. Gingeras, B. Fazekas de St Groth, et al. 2006. CD127 expression inversely correlates with FoxP3 and suppressive function of human CD4+ T reg cells. *J. Exp. Med.* 203: 1701–1711.
27. Seddiki, N., B. Santner-Nanan, J. Martinson, J. Zaunders, S. Sasson, A. Landay, M. Solomon, W. Selby, S. I. Alexander, R. Nanan, et al. 2006. Expression of interleukin (IL)-2 and IL-7 receptors discriminates between human regulatory and activated T cells. *J. Exp. Med.* 203: 1693–1700.
28. Dunham, R. M., B. Cervasi, J. M. Brechley, H. Albrecht, A. Weinrobb, B. Sumpter, J. Engram, S. Gordon, N. R. Klatt, I. Frank, et al. 2008. CD127 and CD25 expression defines CD4+ T cell subsets that are differentially depleted during HIV infection. *J. Immunol.* 180: 5582–5592.
29. Getnet, D., J. F. Grosso, M. V. Goldberg, T. J. Harris, H. R. Yen, T. C. Bruno, N. M. Durham, E. L. Hipkiss, K. J. Pyle, S. Wada, et al. 2010. A role for the transcription factor Helios in human CD4(+)CD25(+) regulatory T cells. *Mol. Immunol.* 47: 1595–1600.
30. Ray, J. P., H. D. Marshall, B. J. Laidlaw, M. M. Staron, S. M. Kaech, and J. Craft. 2014. Transcription factor STAT3 and type I interferons are corepressive insulators for differentiation of follicular helper and T helper 1 cells. *Immunity* 40: 367–377.
31. Blackburn, M. J., M. Zhong-Min, F. Caccuri, K. McKinnon, L. Schifanella, Y. Guan, G. Gorini, D. Venzon, C. Fenizia, N. Binello, S. N. Gordon, C. J. Miller, G. Franchini, and M. Vaccari. 2015. Regulatory and helper follicular T cells and antibody avidity to simian immunodeficiency virus glycoprotein 120. *J. Immunol.* 195: 3227–3236.
32. Sage, P. T., L. M. Francisco, C. V. Carman, and A. H. Sharpe. 2013. The receptor PD-1 controls follicular regulatory T cells in the lymph nodes and blood. *Nat. Immunol.* 14: 152–161.
33. Birzele, F., T. Fauti, H. Stahl, M. C. Lenter, E. Simon, D. Knebel, A. Weith, T. Hildebrandt, and D. Mennerich. 2011. Next-generation insights into regulatory T cells: expression profiling and FoxP3 occupancy in Human. *Nucleic Acids Res.* 39: 7946–7960.
34. Moreno-Fernandez, M. E., W. Zapata, J. T. Blackard, G. Franchini, and C. A. Chougnet. 2009. Human regulatory T cells are targets for human immunodeficiency Virus (HIV) infection, and their susceptibility differs depending on the HIV type 1 strain. *J. Virol.* 83: 12925–12933.
35. Brechley, J. M., B. J. Hill, D. R. Ambrozak, D. A. Price, F. J. Guenaga, J. P. Casazza, J. Kuruppu, J. Yazdani, S. A. Migueles, M. Connors, et al. 2004. T-cell subsets that harbor human immunodeficiency virus (HIV) in vivo: implications for HIV pathogenesis. *J. Virol.* 78: 1160–1168.
36. Brechley, J. M., C. Vinton, B. Tabb, X. P. Hao, E. Connick, M. Paiardini, J. D. Lifson, G. Silvestri, and J. D. Estes. 2012. Differential infection patterns of CD4+ T cells and lymphoid tissue viral burden distinguish progressive and nonprogressive lentiviral infections. *Blood* 120: 4172–4181.

Corrections

Chowdhury, A., P. M. E. Del Rio, G. K. Tharp, R. P. Tribble, R. R. Amara, A. Chahroudi, G. Reyes-Teran, S. E. Bosinger, and G. Silvestri. 2015. Decreased T follicular regulatory cell/T follicular helper cell (T_{FH}) in simian immunodeficiency virus–infected rhesus macaques may contribute to accumulation of T_{FH} in chronic infection. *J. Immunol.* 195: 3237–3247.

The second author's name was incorrect in the published article. The correct name is Perla Mariana Del Rio Estrada.

www.jimmunol.org/cgi/doi/10.4049/jimmunol.1502269